Simulation evidence for lateral excitation transfer in a self-assembled quantum-dot array

H. T. Johnson[a] and R. Bose
Department of Mechanical and Industrial Engineering, University of Illinois at Urbana-Champaign, Urbana, Illinois 61801

H. D. Robinson[b] and B. B. Goldberg
Department of Physics, Boston University, Boston, Massachusetts, 02215

(Received 20 November 2002; accepted 19 March 2003)

Simulations of InAlAs/AlGaAs self-assembled quantum-dot arrays containing as many as 30 individual dots are used to identify a mechanism for lateral excitation transfer through partially delocalized heavy-hole states. Individual hole states exhibit wave-function splitting between several dots in the array, as well as partial confinement in the wetting layer, and have strong overlap with multiple conduction-band electron states in different quantum dots. Electron–hole pair energies involving these partially delocalized hole states correspond well with narrow resonances seen in the experimental photoluminescence excitation spectra taken for similar quantum-dot arrays using low-temperature near-field scanning optical microscopy. © *2003 American Institute of Physics.*
[DOI: 10.1063/1.1575509]

Quantum-dot (QD) electronic structure theory[1] is a well-developed field and has resulted in a number of important observations that have helped interpret experimental data. Nearly all theory and simulation studies have focused on individual, idealized QDs. In this letter however, a QD array system consisting of approximately 30 dots of varying size and shape is studied. By considering a full array of dots, it is possible to address the issue of lateral interdot excitation transfer studied experimentally using near-field scanning optical microscopy (NSOM).

A finite element computational mesh for the system under consideration is shown in Fig. 1. It consists of an array of approximately 30 $In_{0.55}Al_{0.45}As$ QDs on a substrate of $Al_{0.35}Ga_{0.65}As$, and buried by a capping layer of the same material. An experimental system consisting of the same materials has been extensively studied previously.[2–7] In both simulations and experiments, the average dot diameter is ~18 nm. The wetting layer thickness varies, but averages ~3 nm, and the interdot spacing is slightly larger than the average dot diameter.

Robinson *et al.*[7] found evidence for interdot excitation transfer in low-temperature near-field photoluminescence excitation (PLE) experiments. The sample is excited in illumination-mode NSOM at 4 K with a tip small enough to excite as few as 10–25 dots (~100 nm). The lateral diffusion of excitons is limited by exciting below the wetting-layer (WL) exciton energy. The emission signal is collected using conventional far-field optics. Figure 2 shows that at specific excitation energies, the emission of several neighboring QDs is simultaneously and resonantly enhanced indicating some mechanism of lateral excitation transfer or coupling. They suggested that multiple dots with different emission energies are simultaneously excited due to coupling between localized states in the WL, or alternatively, through Förster dipole energy transfer. In contrast, this letter describes direct simulation evidence for resonant multidot emission through delocalized hole states.

A simple computational model is used to consider the optical emission spectrum of the QD array system shown in Fig. 1. The general finite element approach, using a strain-modified **k·p** Hamiltonian to compute single electron energies, is described in detail elsewhere.[8] With conduction-band and heavy-hole (hh) energies and wave functions, the energies and relative intensities of optical transitions can be evaluated to leading order by computing overlap integrals of all possible electron–hole pairs. Several important approximations—most notably the neglect of exciton binding energy effects—limit the detailed energy accuracy of the method, but the approach captures the basic self-assembled QD array electronic and optical properties.[9] Furthermore, the relatively large size of the system makes a more accurate atomistic method computationally unfeasible.

Results of the finite element solution for the electron and hole energies and wave functions for the system shown in Fig. 1 include primarily the separate *s*-type and *p*-type states

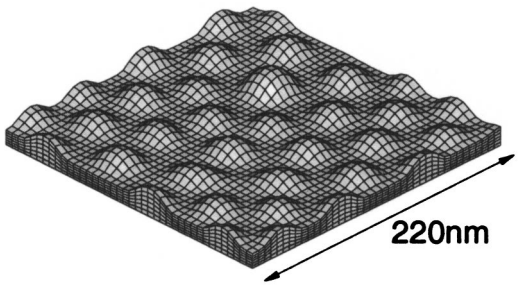

FIG. 1. The computational mesh used in the simulation. The domain includes approximately 30 QDs, with an average dot diameter of approximately 18 nm. Symmetry conditions are used at the lateral boundaries. Capping layer elements are not shown.

[a]Electronic mail: htj@uiuc.edu
[b]Current address: Department of Electrical Engineering, University of California at Los Angeles, Los Angeles, California, 90095.

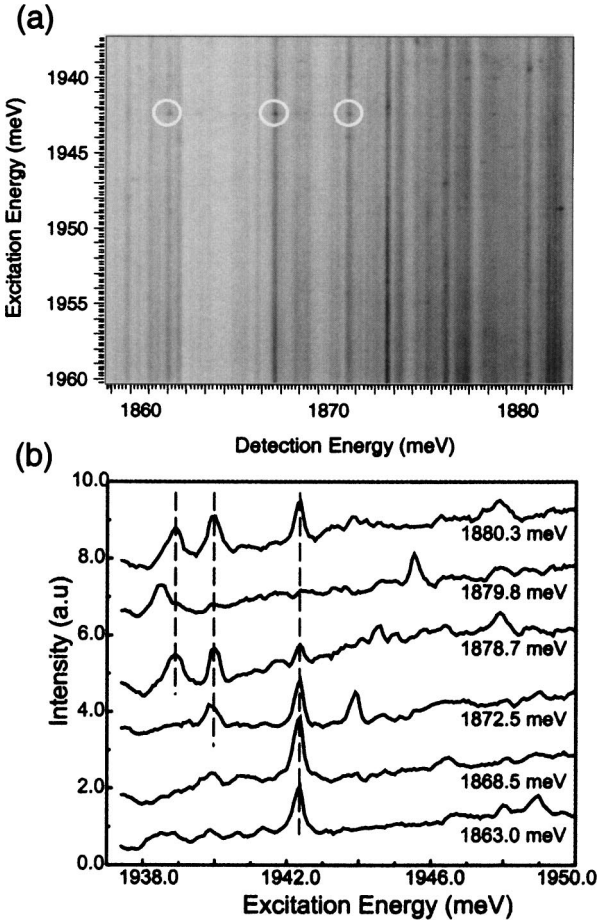

FIG. 2. Resonances in the low-temperature near-field PLE spectra for the QD array (adapted from a figure in Ref. 7). (a) QD emission in reverse gray scale showing several intensity peaks resonantly enhanced at particular excitation energies. (b) Individual vertical line cuts showing resonant enhancement [from a different data set than (a)].

associated with each of the dots in the array. Figure 3 shows a section of the computational domain with probability densities for the lowest two conduction-band energy states in the 30 dot system: the *s*-type and first *p*-type state for the largest dot.

Permissible interband optical transitions from the computed electron and hole states with large spatial overlap are represented graphically in Fig. 4. Each point represents an interband optical transition for the system, with the participating conduction-band state along the horizontal and hh state along the vertical axis. The magnitude of the overlap ($\langle i|j\rangle$) is represented by the intensity in reverse gray scale, which can be interpreted as the relative intensity of the transition. The optical transition energies, or sum of electron and hole energies, are in the range of the detection and excitation energies probed in the experiments summarized in Fig. 2. Furthermore, the average energy splitting between ground state conduction-band electrons and first and second excited conduction electrons, 36 and 69 meV, are in excellent agreement with experimental data.[2–7]

The overlap diagram provides a graphical interpretation of the mechanism identified for lateral excitation transfer. While most of the optical transitions fall along the diagonal streaks in the diagram, there are several faint but visible interband transitions occurring along a horizontal. Points in

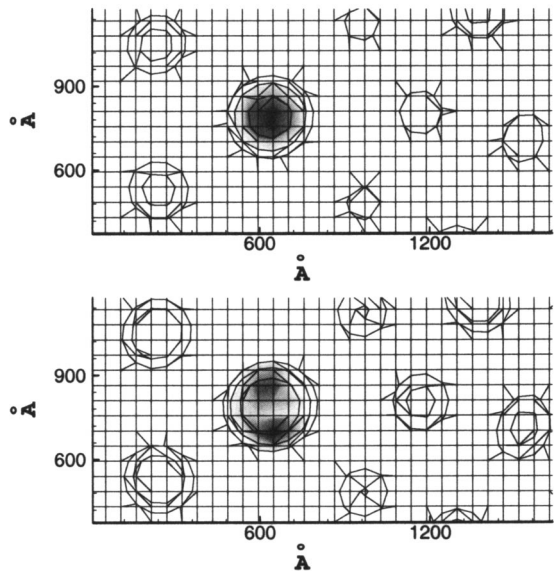

FIG. 3. Probability densities for the two lowest conduction-band states in the system, an s-type state in the largest dot (above) and a p-type state in the same dot (below). The plot is taken on surfaces of fixed height in the growth direction. Other smaller dots surround the larger dot in the array, but the wave function is strongly confined to the large dot.

line horizontally represent overlap between a single hh state and a number of conduction-band electron states, including *s*-type states in different dots, ground and excited states in the same dot, or a combination of these.

The probability density for such a hh state, corresponding to the middle of the three highlighted horizontals in Fig. 4, is shown in Fig. 5 (upper left). The state is clearly partially delocalized between multiple separate QDs; the calculations show that the wave function spreading between the dots is mediated by the WL. Also shown in Fig. 5 are the conduction-band electron states that the partially delocalized hh state overlaps.

Lateral excitation transfer through such a partially delo-

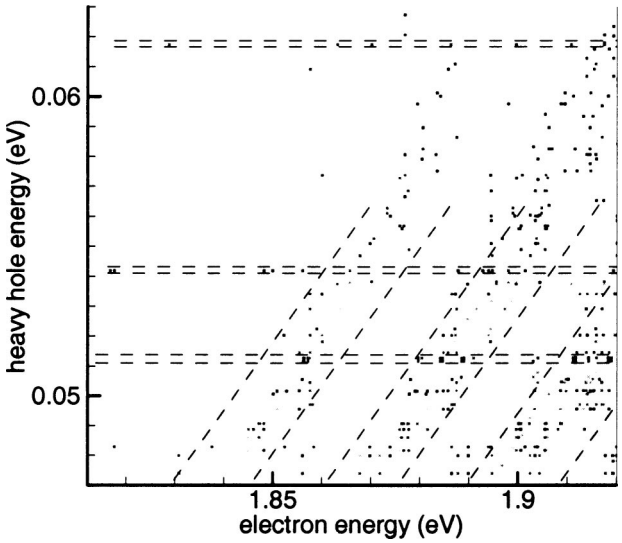

FIG. 4. Overlap diagram for interband optical transitions based on the computed conduction and hh states. The three diagonal streaks identified by dashed lines represent the overlap with hhs by ground state conduction electrons, first excited conduction electrons, and second excited conduction electrons, respectively. Horizontal streaks identified by dashed lines are due to partially delocalized hhs.

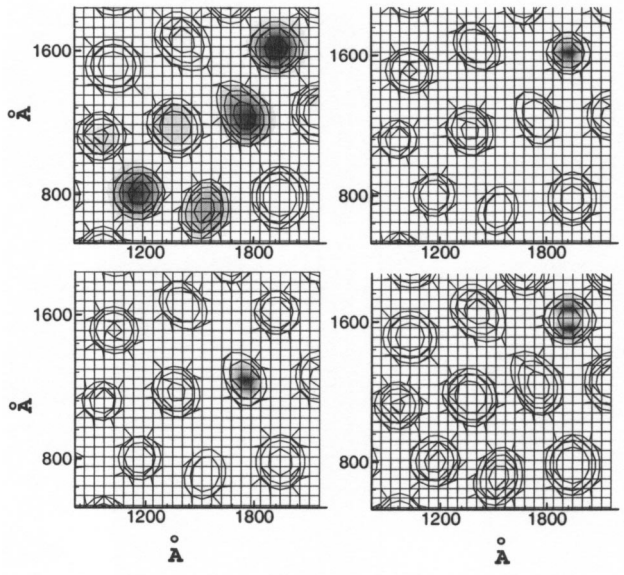

FIG. 5. Hh (upper left) and electron states involved in the lateral excitation transfer mechanism. The excitation energy is resonant with the energy difference between the hole state (upper left) and an excited conduction state (lower right). Emission then occurs from multiple dots with ground conduction states (upper right, lower left) spatially connected via the hh state.

calized hh state can be explained as follows. The PLE excitation laser is tuned to the energy difference associated with the (partially delocalized) hh and (first or second excited) conduction electron pair in a particular dot. Emission occurs then between the partially delocalized hh state paired with the ground conduction electron state in the same dot. Simultaneously, excitation transfers to a different dot or dots through the partially delocalized hh state, and emission occurs between the hh state and the ground state of the other dots involved. The hh state shown in Fig. 5 would lead to at least three resonant peaks. Representative conduction-band states associated with two of these are also shown in Fig. 5. Emission due to the nonzero overlap between WL electron states and delocalized hole states is ruled out as an explanation for the resonant peaks because the computed energy difference between states falls far outside the experimentally measured values.

Note that due to the band alignment of the materials in the structure, the electron states are too strongly confined or localized (with confinement energies of 0.4 ± 0.05 eV due to local strain effects) to allow such resonant (excitonic) transfer. The hhs, by comparison, are very weakly confined by the shallow potential well (0.1 ± 0.05 eV) associated with the valence-band offset. Due to the high excitation densities in the near-field, a significant nonresonant emission is seen in the QDs, displayed by the continuous vertical lines in Fig. 2, which is adapted from a figure published in Ref. 7. This nonresonant dot excitation provides the necessary electrons for recombination in the transferred dots.

The overlap ($\langle i|j\rangle$) for the combinations shown in Fig. 5 varies from 0.05 to 0.10, compared to the 0.3 to 0.4 overlap computed for a standard *s*-type hh and *s*-type conduction-band pair, multiple examples of which are represented in the leftmost diagonal streak in Fig. 4. The ~20%–30% extra intensity in experimentally observed resonant emission [shown in Fig. 2(b)] may be explained by one or a few resonant dots serving as extra channels and contributing 0.05–0.10 in intensity to the 0.3–0.4 of the main dot. This small additional resonant intensity is unlike the orders of magnitude enhancements associated with other types of resonance phenomena. Furthermore, the energy separation between such resonances at a given excitation energy varies from as little as several tenths meV to 10 meV, depending on the variation in QD size among the dots involved in the resonance. This is also consistent with the experimentally observed resonances.

The partially delocalized hh states involved in the resonances are identified as a natural consequence of the nonuniformity of the mesh used in the finite element **k·p** Hamiltonian calculation. For example, the WL thickness varies slightly between different regions of the QD array, and individual dots have varying shape, size, and spacing. Thus, consideration of the full QD array is necessary to identify such a mechanism. Here, it offers clear support to the idea of lateral excitation transfer suggested in the experiments of Robinson *et al.*

The authors wish to thank Prof. A. Bower of Brown University for providing the computational mesh from the results of his morphology simulations.[10] The support of NSF Grant Nos. CMS-0296102 and DMR-9701958 is gratefully acknowledged.

[1] A. Zunger, Phys. Status Solidi B **224**, 727 (2001).
[2] S. Fafard, R. Leon, J. L. Merz, and P. M. Petroff, Phys. Rev. B **52**, 5752 (1995).
[3] R. Leon, S. Fafard, D. Leonard, J. L. Merz, and P. M. Petroff, Science (Washington, DC, U.S.) **267**, 1966 (1995).
[4] R. Leon, S. Fafard, D. Leonard, J. L. Merz, and P. M. Petroff, Appl. Phys. Lett. **67**, 521 (1995).
[5] P. D. Wang, J. L. Merz, S. Fafard, R. Leon, D. Leonard, G. Medeiros-Ribeiro, M. Oestrich, P. M. Petroff, K. Uchida, N. Miura, H. Akiyama, and H. Sakaki, Phys. Rev. B **53**, 16458 (1996).
[6] H. D. Robinson, M. G. Müller, B. B. Goldberg, and J. L. Merz, Appl. Phys. Lett. **72**, 2081 (1998).
[7] H. D. Robinson, B. B. Goldberg, and J. L. Merz, Phys. Rev. B **64**, 075308 (2001).
[8] H. T. Johnson, C. D. Akyüz, L. B. Freund, A. Zaslavsky, J. Appl. Phys. **84**, 3714 (1998).
[9] H. T. Johnson, V. Nguyen, and A. F. Bower, J. Appl. Phys. **92**, 4653 (2002).
[10] Y. Zhang and A. F. Bower, J. Mech. Phys. Solids **47**, 2273 (1999).